



# report

IVL Swedish Environmental Research Institute

## High and low NO<sub>x</sub> chemistry in the troposphere

Implementing the use of indicator species in a trajectory model

Johanna Altenstedt  
B 1301  
Göteborg, June 1998

<p><b>Organisation/Organization</b>  Institutet för Vatten- och Luftvårdsforskning</p> <p><b>Adress/Address</b>  Box 47086  402 58 GÖTEBORG</p> <p><b>Telefonnr/Telephone</b>  031-48 21 80</p>	<p><b>RAPPORTSAMMANFATTNING</b>  <b>Report Summary</b></p> <p><b>Projekttitel/Project title</b>  Modelling of the high to low NO<sub>x</sub> transition using the IVL model - a contribution to the EUROTRAC sub-project LOOP</p> <p><b>Anslagsgivare för projektet/Project sponsor</b>  Naturvårdsverket</p>
<p><b>Rapportförfattare, author</b>  Johanna Altenstedt</p>	
<p><b>Rapportens titel och undertitel/Title and subtitle of the report</b>  High and low NO<sub>x</sub> chemistry in the troposphere  Implementing the use of indicator species in a trajectory model</p>	
<p><b>Sammanfattning/Summary</b>  Ground level ozone is considered to be an important environmental threat affecting human health negatively and causing damage to vegetation. Ozone is produced from nitrogen oxides (NO<sub>x</sub>) and volatile organic compounds (VOC) in the presence of sunlight. The only way to reduce ozone is to reduce the emissions of the precursors. There are two different chemical states in the troposphere, referred to as low and high NO<sub>x</sub> chemistry. In the low NO<sub>x</sub> areas, the ozone is limited by the availability of NO<sub>x</sub>, while in the high NO<sub>x</sub> areas, it is the VOC which limits the production of ozone. The use of indicator species, as a way to decide the chemical state the troposphere, has been investigated using the IVL trajectory model. The concept has previously been tested for US conditions in a 3D model. The study show that the concept of indicator species can be implemented in a trajectory model. The values of the indicator species for the transition from high to low NO<sub>x</sub> have been estimated for European conditions and have shown a reasonable agreement with the previous findings in the US.</p>	
<p><b>Nyckelord samt ev. anknytning till geografiskt område, näringsgren eller vattendrag/Keywords</b>  Ozone, troposphere, NO<sub>x</sub>, VOC, indicator species, emission reductions</p>	
<p><b>Bibliografiska uppgifter/Bibliographic data</b>  <b>IVL Rapport B-1301</b></p>	
<p><b>Beställningsadress för rapporten/Ordering address</b>  IVL, Publikationsservice, Box 21060, S-100 31 Stockholm</p>	

# Table of contents

<b>1. Introduction</b>	<b>1</b>
1.1. <i>The photostationary state</i>	2
1.2. <i>Low and high NO<sub>x</sub> chemistry</i>	2
1.3. <i>Indicator species</i>	3
1.4. <i>Contribution to the LOOP project (Limitation Of Oxidant Production)</i>	4
<b>2. Model set-up and simulations</b>	<b>6</b>
2.1. <i>Comparing indicator species in 3D and 1D models</i>	6
2.2. <i>The IVL photochemical trajectory model</i>	6
2.3. <i>Meteorology</i>	8
2.4. <i>Initial concentrations</i>	9
2.5. <i>Dry deposition</i>	10
2.6. <i>Emissions</i>	10
2.7. <i>Simulation scenarios</i>	13
<b>3. Results and discussion</b>	<b>15</b>
3.1. <i>Total ozone concentration</i>	15
3.2. <i>Changes in ozone due to emission reductions</i>	18
3.2.1. <i>Average changes in ozone</i>	18
3.2.2. <i>Changes in maximum ozone concentration</i>	19
3.2.3. <i>Changes in ozone from emission reductions, with biogenic emissions present</i>	22
3.3. <i>Indicator species</i>	23
3.3.1. <i>The indicator species NO<sub>y</sub></i>	23
3.3.2. <i>The indicator species O<sub>3</sub>/(NO<sub>y</sub>-NO<sub>x</sub>)</i>	25
3.3.3. <i>The indicator species HCHO/NO<sub>y</sub></i>	26
3.3.4. <i>The indicator species H<sub>2</sub>O<sub>2</sub>/HNO<sub>3</sub></i>	27
3.3.5. <i>Values for indicator species on different days along a trajectory</i>	28
3.3.6. <i>Values for indicator species when biogenic emissions are present</i>	29
<b>4. Conclusions</b>	<b>30</b>
<b>5. Acknowledgements</b>	<b>32</b>
<b>6. References</b>	<b>33</b>

# 1. Introduction

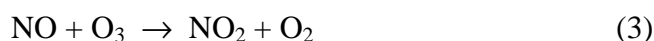
Ozone is produced close to the ground from nitrogen oxides ( $\text{NO}_x$ ) and volatile organic compounds (VOC) in the presence of sunlight. The elevated concentration of tropospheric ozone presents a threat to human health and causes damage to vegetation. Both the occurrence of high concentrations of photooxidants as well as high cumulative ozone doses during longer time periods need to be reduced by decreasing the emissions of the precursors. Ozone is also a greenhouse gas, which adds to the greenhouse effect.

$\text{NO}_x$  and VOC are emitted into the atmosphere from both anthropogenic and biogenic emission sources. The ozone formation is governed by the amount of available  $\text{NO}_x$  and VOC but there is no simple relation to describe the connection between the rate of ozone production and the amount of precursors in the atmosphere. The complexity of the ozone formation processes makes it difficult to identify the most cost effective measures to take towards ozone reduction (Lin et al, 1988; Bowman and Seinfeld, 1994; Altshuler et al., 1995). Abatement strategies to reduce the levels of ozone could include reductions in both  $\text{NO}_x$  and VOC emissions depending on the specific chemical environment where the reductions are to be carried out. The emissions of  $\text{NO}_x$  and VOC varies frequently in Europe (Mylona, 1996) which makes abatement strategy decisions very difficult. A more detailed knowledge of the non-linear chemical generation processes of ozone and other photooxidants in the atmosphere under European conditions is therefore much desired.

Along with measurements and emission inventories, atmospheric models play an important part in the work to reduce ozone. Atmospheric models simulate the transport of air and the chemical reactions which take place in the atmosphere. There are a variety of different models focusing on different aspects of the atmosphere. Some are focusing on the meteorology of the atmosphere and describe the transport of air in great detail while others are more chemically detailed. There is not yet one single model which in itself describes the atmosphere absolutely accurate. Several different types of models are therefore often used in connection with one another in abatement strategy work.

## 1.1. The photostationary state

Ground level ozone is formed from nitrogen oxides ( $\text{NO}_x$ ) and VOC under the influence of sunlight. The reaction which produces ozone ( $\text{O}_3$ ) in the troposphere is the photolysis of nitrogen dioxide ( $\text{NO}_2$ ), which produces nitric oxide (NO) and atomic oxygen ( $\text{O}({}^3\text{P})$ ). Atomic oxygen combines with an oxygen molecule ( $\text{O}_2$ ) to form ozone. Ozone can oxidise nitric oxide to nitrogen dioxide and together these reactions form a steady state between ozone, nitric oxide and nitrogen dioxide referred to as the photostationary state (reactions 1-3).



If no VOC were present in the atmosphere, the photostationary state would govern the background levels of ozone. When VOC are introduced into the troposphere they are oxidised to produce peroxy radicals. Peroxy radicals can either consume NO or convert it to  $\text{NO}_2$  and thereby compete with ozone in the photostationary state. Less ozone is thereby destroyed through reaction with NO (reaction 3) and hence the ozone concentration increases.

$\text{NO}_x$  is not consumed in the photostationary state but is regenerated and thus acts as a catalyst (reactions 1-3). Organic compounds on the other hand act as the fuel for ozone production and are consumed in the process.

## 1.2. Low and high $\text{NO}_x$ chemistry

There are two different states of the atmosphere which are usually referred to as the low and high  $\text{NO}_x$  regimes. In the low  $\text{NO}_x$  regime the production of ozone is mainly governed by the amount of  $\text{NO}_x$ , while in the high  $\text{NO}_x$  regime the amount of ozone which is produced is controlled both by the  $\text{NO}_x$  and VOC levels (Sillman *et al.*, 1990; Chameides *et al.*, 1992). Urban areas are generally in the high  $\text{NO}_x$  regime while rural areas are in the low  $\text{NO}_x$  regime.

In many parts of Europe areas in the low  $\text{NO}_x$  regime are close to areas in the high  $\text{NO}_x$  regime and therefore abatement strategy work becomes complicated. The transition between the low and high  $\text{NO}_x$  regime is thus an area which needs further

investigation, especially for European conditions. In plumes from highly polluted urban areas in Scandinavia, e.g. Stockholm, Göteborg, Malmö/Köpenhamn and Stenungsund, a transition from high to low NO<sub>x</sub> regime inevitably takes place as the plume moves into more rural areas surrounding the city.

Either of the two precursors may limit the rate of ozone production (PO<sub>3</sub>). Reducing the emissions of the limiting precursor will reduce ozone whereas reduction of the other precursor emissions will have little effect on the ozone concentration. In areas which are already rich in NO<sub>x</sub> emissions, an additional source of NO<sub>x</sub> will decrease the ozone concentration, due to the fast reaction between ozone and NO (reaction 3). This effect may last over a large geographical scale, if the NO<sub>x</sub> emissions from the area are maintained on a high level. Approximations of PO<sub>3</sub> as a function of NO<sub>x</sub> and VOC have been presented elsewhere (Sillman et al., 1990), as shown in equation 4.

In order to define the effectiveness of a reduction strategy the chemical state has to be known. The transition can be defined as the point where a relative decrease in both NO<sub>x</sub> and VOC emissions has the same effect on PO<sub>3</sub>.

$$\frac{\partial PO_3}{\partial [VOC]} \cdot [VOC] = \frac{\partial PO_3}{\partial [NO_x]} \cdot [NO_x] \quad (4)$$

This approach has been used to define indicator species (Table 1.1). that allow to distinguish between chemical states for which VOC or NO<sub>x</sub> reductions are more efficient (Sillman, 1995). These indicators were evaluated for Eastern USA (Sillman, 1995). We will evaluate the validity of these numbers for the area under investigation.

### **1.3. Indicator species**

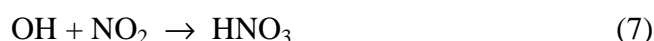
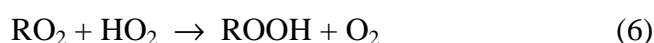
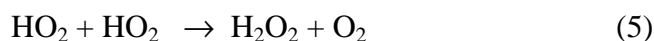
The indicators have already been evaluated for US conditions (Sillman, 1995) and the need for modifications to suit European conditions will be assessed.

**Table 1.1.** Indicator species for NO<sub>x</sub> and VOC sensitivity (Sillman, 1995).

Indicator species	NO <sub>x</sub> sensitive	VOC sensitive
NO <sub>y</sub>	< 20 ppb	> 20 ppb
O <sub>3</sub> /(NO <sub>y</sub> - NO <sub>x</sub> )	> 7	< 7
HCHO/NO <sub>y</sub>	> 0.28	< 0.28
H <sub>2</sub> O <sub>2</sub> /HNO <sub>3</sub>	> 0.4	< 0.4

Ozone formation in air masses over rural areas in Europe is often limited by the availability of NO<sub>x</sub> during summer time. By passing over an urban area the high emission densities of NO<sub>x</sub> and VOC can shift the regime towards VOC sensitive ozone production. Leaving the urban area, the shorter lifetime of NO<sub>x</sub> and dilution leads to a faster depletion of NO<sub>x</sub> compared to VOC and the chemical regime passes the transition to NO<sub>x</sub> sensitive chemistry (Staffelbach and Neftel, 1996). Therefore, it is important to know the temporal evolution and the spatial extent of the different chemical states and the corresponding oxidant production in order to assess the effectiveness of reduction strategies.

Sillman defines the transition between VOC and NO<sub>x</sub> sensitivity based on the relative size of the different reactions which terminate odd hydrogen (OH + HO<sub>2</sub> + RO<sub>2</sub>). The most important of these reaction are reactions 5 to 7 below.



If reaction 7 is the major sink for odd hydrogen then the atmosphere is VOC sensitive but if reactions 5 and 6 are the dominating reactions, the atmosphere is NO<sub>x</sub> sensitive, according to Sillman (1995).

#### **1.4. Contribution to the LOOP project (Limitation Of Oxidant Production)**

The LOOP project is a EUROTRAC-2 subproject which focuses on the transition between high and low NO<sub>x</sub> chemistry in the atmosphere. The chemically detailed IVL model will act as a chemical reference for other less detailed models which take part in the project. The project also provides the opportunity to validate the IVL model against measuring data for a complex but realistic European plume.

The LOOP project uses the area between Milan and the Alps as a natural laboratory to study the oxidation of the emitted species under highly variable conditions. Measurements will provide data for atmospheric models which will be used to investigate the spatial extent of the different chemical regimes of the oxidant formation in the troposphere. Within the project, the Milan urban plume will be examined and the atmospheric indicator species defined by Sillman (1995) (Table 1.1.) will be studied during the transition from high to low  $\text{NO}_x$  in order to establish at what point the transition occurs.

The overall aim of the LOOP project is to increase our knowledge about the transition between high and low  $\text{NO}_x$  atmospheric chemistry and the concept of indicator species is only one way to describe this transition which will be employed within the project.

The work presented in this report has investigated the use of the Sillman indicator species in a 1D IVL trajectory model, under European conditions. The aim has been to see how the indicator species work in this type of model and also to determine whether the transition values calculated for US conditions are applicable also for European conditions.



## **2. Model set-up and simulations**

The transition between low- and high-NO<sub>x</sub> chemistry, and the idea of indicator species to determine this transition, has been investigated through model simulations for European conditions. The IVL-model, a two layer Lagrangian photochemical model which describes an air mass as it moves along a trajectory in the atmospheric boundary layer, has been employed in the investigation (Pleijel and Andersson-Sköld, 1992).

### **2.1. Comparing indicator species in 3D and 1D models**

The idea of using indicator species to describe the transition from high- to low-NO<sub>x</sub> chemistry means that the current values of the different indicator species are recorded along with the reduction in ozone. When Sillman investigated the transition between high- and low-NO<sub>x</sub> chemistry for US conditions, through the use of indicator species, he used a 3D-model (Sillman, 1995). A 3D-model can be described as a large number of boxes of air which are connected to each other, but which all experience different emissions. In a trajectory model, which have been used in this study, a simulation can only describe one emission scenario at a time. To reproduce the results from a 3D-model, several individual trajectories need to be simulated. For each scenario separate reductions in NO<sub>x</sub> and VOC need to be performed and the reduction in ozone are then recorded at the same time in each scenario.

In this investigation we aim to describe a large range of emissions scenarios to represent the varying conditions within Europe. The model has been developed to suit Swedish conditions and therefore many of the parameters which are specified in the sections below are based on the conditions in southern Sweden. It is however complicated to vary to many parameters at the same time and the differences between the various scenarios have therefore been limited to only the emissions of NO<sub>x</sub> and VOC (together with CO).

### **2.2. The IVL photochemical trajectory model**

The IVL model describes the chemical development in an air mass as it experiences emissions, deposition and mixing in of above air along a trajectory. The model was originally developed at Harwell (Derwent and Hov, 1979; Derwent and Hough, 1988)

but has at IVL been chemically expanded and revised to fit Swedish conditions (Pleijel *et al.*, 1992; Andersson-Sköld *et al.*, 1992). The IVL-model includes the explicit decomposition of around 80 of the most common VOC in Europe. It contains more than 700 species taking part in over 2000 chemical reactions (Andersson-Sköld, 1995). The model is one of the most chemically detailed photochemical models in Europe and have been used in many comparison studies, most recently in the EUROTRAC model intercomparison study (Kuhn *et al.*, 1998).

The lower layer of the model describes the boundary layer while the above layer represents the free troposphere. The height of the boundary layer is during the night kept at its minimum value. One hour after sunrise the boundary layer starts to expand, mixing in air from the free troposphere above. The boundary layer reaches its maximum height at 2 p.m. and thereafter stays constant during the rest of the sunlit hours of the day. At sunset, the boundary layer collapses down to its minimum height and at the same time the concentrations of the free troposphere is set to the concentrations in the boundary layer in the model.

The rate expressions,  $dC_i/dt$ , for each species within the model describes the chemical development within each layer of the model. For a species  $i$  in the boundary layer, the differential equation which represents the concentration development in time,  $C_i$ , will be expressed as in equation 8 below.

$$\frac{dC_i}{dt} = P_i - L_i C_i - \frac{V_{i,g} C_i}{h} + \frac{E_i}{h} - \frac{(C_i - C_{i,n})}{h} \cdot \frac{dh}{dt} \quad (8)$$

where:

- $C_i$  is the concentration of species  $i$  in [molecules · cm<sup>-3</sup>] in the boundary layer,
- $P_i$  is the chemical production rate in [molecules · cm<sup>-3</sup> · s<sup>-1</sup>] for species  $i$ ,
- $L_i$  is the chemical loss rate coefficient in [s<sup>-1</sup>] for species  $i$ ,
- $V_{i,g}$  is the dry deposition rate in [cm · s<sup>-1</sup>] for species  $i$ ,
- $h$  is the height of the mixing layer in [cm],
- $E_i$  is the emission rate in [molecules · cm<sup>-2</sup> · s<sup>-1</sup>] for species  $i$ ,
- $C_{i,n}$  is the concentration of species  $i$  in [molecules · cm<sup>-3</sup>] in the air layer above the boundary layer. The second last term, represents the mixing in of air into the boundary layer from the layer above.

For the upper layer, which experiences neither emissions nor dry deposition and which is not affected by any adjacent layer of air, only the first two terms on the right hand side of the continuity equation above, apply.

The differential equations were solved using the calculation program FACSIMILE (AEA Technology, 1995), employing Gear's method (Gear, 1969) on a Sun Workstation.

### 2.3. Meteorology

The production of ozone is highly dependent on the solar irradiance and the highest concentrations of ozone are obtained when the solar irradiance is high. For these simulations the meteorological parameters are chosen to reflect weather conditions which are favourable for ozone production, i.e. an ozone episode. This is represented by a cloudfree high pressure situation with light winds in the middle of the summer. The diurnal variation of the solar radiation at the 28th of May was used since it is fairly close to midsummer, when the solar radiation reaches its maximum. The reason for not choosing a date in the middle of the summer is that the chosen date is more representative for the growing season. The latitude was chosen to be 58°N which corresponds to Gothenburg in southern Sweden, and the diurnal variations of wind speed, relative humidity and air temperature have been based on around 30 years of weather statistics for southern Sweden (Taesler, 1972). In the model, these parameters are assumed to follow the solar angle during the sunlit hours, whilst during the hours of darkness they are set to constant values. Clouds are in the model assumed to only reduce the solar radiation below them, but in these simulations this has not been applied since the cloudiness has been set to zero. The meteorological parameters used in these simulations are all shown in Table 2.1. below.

**Table 2.1.** The meteorological parameters used in the model simulations.  $\Theta$  = the solar angle.  $\sin \Theta$  is set to zero if it is lower than 0.001, i.e. during the night.

<b>Date</b>	28th of May
<b>Latitude</b>	58°N
<b>Boundary layer (min)</b>	150 [m]
<b>Boundary layer (max)</b>	1000 [m]
<b>Wind speed</b>	$2 + 1.5 \sin\Theta$ [ $\text{m}\cdot\text{s}^{-1}$ ]
<b>Temperature</b>	$287.2 + 8.3 \sin\Theta$ [K]
<b>Relative humidity</b>	$78 - 26 \sin\Theta$ [%]
<b>Cloudiness</b>	0/8

## 2.4. Initial concentrations

The simulations were conducted for several hypothetical air masses, all experiencing different emissions of anthropogenic NO<sub>x</sub>, VOC and CO. The initial concentrations of ozone, nitrogen oxides and volatile organic compounds, were despite this set to constant values for all the simulations in order to minimise the number of varying parameters. The concentrations used at the start of the simulation, were obtained from the Swedish TOR station situated at Rörvik on the Swedish west coast (Lindskog, 1996) and represents a polluted air mass which has passed over western Europe before reaching Sweden (Janhäll *et al.*, 1995). The concentration of ozone was set to a higher value than the measured in order to reflect the generally more polluted European situation (Lindskog, 1997). The initial concentrations used in this study are collected in Table 2.2 below.

**Table 2.2.** Initial concentrations used in the model (Janhäll *et al.*, 1995; Lindskog, 1997).

Species	Initial concentration (ppb)
ozone	70
NO <sub>2</sub>	4.6
NO	0.92
ethane	1.27
acetylene	0.45
propane	0.43
i-butane	0.28
n-butane	0.49
i-pentane	0.29
n-pentane	0.16
ethene	0.29
propene	0.05
1-butene	0.01
1-pentene (incl. 3-methyl-1-butene)	0.01
2-butene	0.01
i-butene	0.31
2-pentene	0.009
2-methyl-1-butene	0.005
2-methyl-2-butene	0.006
methane	1700
CO	200
H <sub>2</sub>	500
PAN	0.35
acetaldehyde	0.25
HNO <sub>3</sub>	0.1
H <sub>2</sub> O <sub>2</sub>	2
SO <sub>2</sub>	2

## 2.5. Dry deposition

Dry deposition of O<sub>3</sub>, HNO<sub>3</sub>, SO<sub>2</sub>, NO<sub>2</sub>, H<sub>2</sub>O<sub>2</sub>, PAN, analogues of PAN, aldehydes and organic peroxides is included in the 1995 version of the IVL model. The deposition of aldehydes, organic hydroperoxides and PAN analogues have in a previous study been shown to have no significant influence on the calculated concentrations of ozone (Altenstedt and Andersson-Sköld, 1995). The deposition of these species has however still been included in the model since the impact which it will have on the calculation of the indicator species is not established. The dry deposition rates are chosen to correspond to the dry deposition over an average Swedish terrain with a 50 % forest coverage. The dry deposition velocities used in the simulations are given as diurnal mean values in Table 2.3 below.

**Table 2.3.** Dry deposition velocities used in the model simulations (Pleijel *et al.*, 1992; Simpson *et al.*, 1993).

Species	V <sub>d</sub> [cm·s <sup>-1</sup> ]
O <sub>3</sub>	0.5
HNO <sub>3</sub>	2.0
NO <sub>2</sub>	0.15
H <sub>2</sub> O <sub>2</sub>	0.5
SO <sub>2</sub>	0.5
PANs	0.2
Aldehydes	0.3
Organic peroxides	0.5

## 2.6. Emissions

The model includes emissions of NO<sub>x</sub>, VOC, CO, SO<sub>2</sub>, CH<sub>4</sub> and isoprene. Emissions of SO<sub>2</sub> has been set to a constant value of 0.64 tonnes·km<sup>-2</sup>·year<sup>-1</sup> in all simulations, which reflects the situation in southern Sweden. The emissions of CH<sub>4</sub>, of which most comes from biogenic sources, has been set to 21.5 tonnes·km<sup>-2</sup>·year<sup>-1</sup> in all simulations. This value is taken from an old emission inventory for Sweden and overestimates the situation in Sweden today (Mylona, 1996). In the scenarios with high VOC emissions this CH<sub>4</sub> emission is of no importance. In the low VOC emission scenarios the initial concentrations of CO (200 ppb) and CH<sub>4</sub> (1700 ppb) is still the same regardless of the VOC emissions. To see whether the rather high emission of

CH<sub>4</sub> could cause any problems in these VOC limited cases some additional simulations of this type of scenarios, but where the emissions of CH<sub>4</sub> were omitted, were performed. These simulations show that the background emissions of CH<sub>4</sub> has no importance even in these cases using the model set-up described above. The distribution of the VOC emitted along the simulated trajectory was taken from a hypothetical air mass transported over Europe (Poppe *et al.*, 1996). The distribution of the VOC used in the model is given in Figure 2.1. together with the VOC distribution for southern Sweden (Janhäll and Andersson-Sköld, 1997) for comparison.

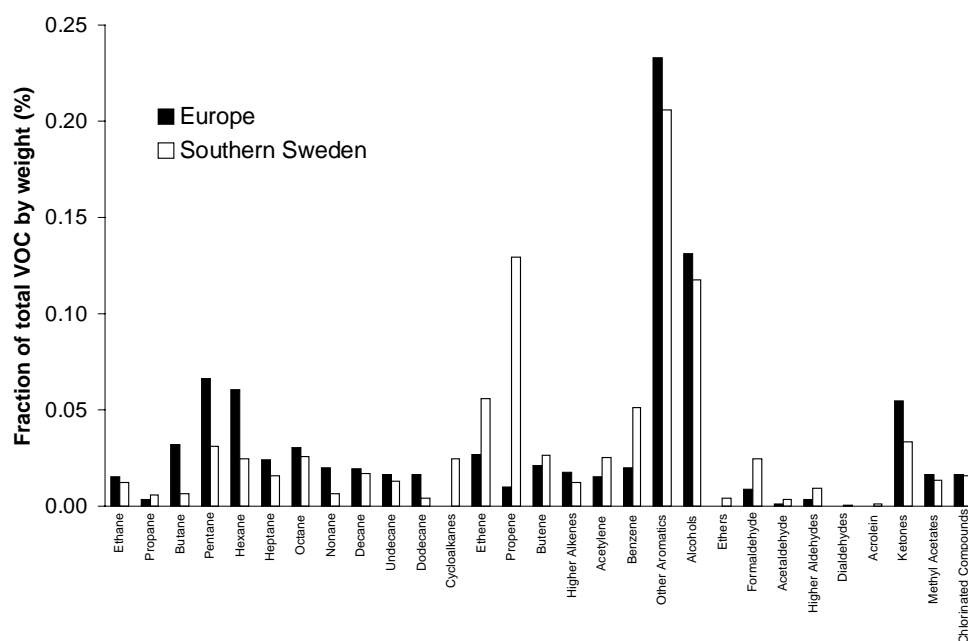


**Figure 2.1.** The distribution of VOC used in the simulations, representing Europe, and the VOC distribution for southern Sweden given for comparison. The distribution is given in % by weight of the total VOC emissions.

The total emissions of NO<sub>x</sub> and VOC were taken from the EMEP emissions inventory. For each square within the EMEP grid the total amount of NO<sub>x</sub> and VOC emissions as well as the ratio of VOC/NO<sub>x</sub> were studied separately. Based upon these data the emissions of both NO<sub>x</sub> and VOC were set to cover a range from 0.03 up to 30 tonnes·km<sup>-2</sup>·year<sup>-1</sup> and the ratio of VOC/NO<sub>x</sub> was set to vary between 0.1 and 100. The CO emission was set to 3.7 times the VOC emissions and was varied along with the current VOC emission for each emission scenario. This relation between the CO and VOC emissions is taken from an old emission inventory for Sweden but correlates well with the ratio between the total European emission of CO and VOC for 1994 (Mylona, 1996). The ratio between the CO and the VOC emissions varies from one country to another within Europe. To test whether the ratio between the CO and VOC

emissions is of great importance some additional simulations of a few scenarios with rather high VOC emissions were rerun with the ratio of CO to VOC set to 2 and 5 instead of 3.7. The results from these simulations show that the amount of CO emissions has some effect on the results and will be discussed later in the results and discussion. The emissions of CO has however been fixed to 3.7 in order to keep the number of varying parameters down. A total of 67 different emission scenarios have been tested and they are visualised in Figure 2.2. below.

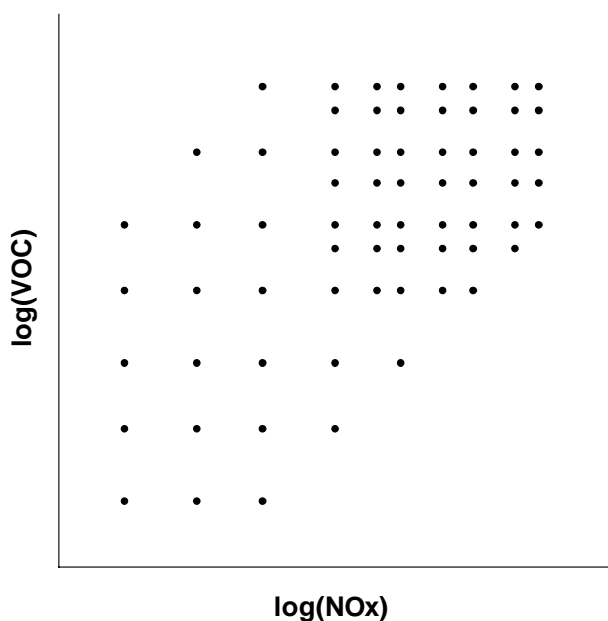


**Figure 2.2.** The different emission scenarios plotted as the logarithm of VOC emission versus the logarithm of  $\text{NO}_x$  emission. Each point refers to a different emission scenario which has been simulated. There are ten different levels of emission rates for both  $\text{NO}_x$  and VOC; 0.03, 0.1, 0.3, 1, 2, 3, 6, 10, 20 and 30 tonnes·km<sup>-2</sup>·year<sup>-1</sup>.

The emissions of  $\text{NO}_x$ , VOC and CO are varied over the day according to rush hour traffic, but besides this variation all emissions are kept constant during the simulations in order to keep the number of variables down.

Three different levels of isoprene emissions have been employed for each of the different emission scenarios; either without any isoprene emissions at all or with isoprene emission of 1.5 or 3 tonnes·km<sup>-2</sup>·year<sup>-1</sup>.

The simulations using the detailed chemical scheme of the IVL model has been complimented with simulations using the less detailed EMEP chemical scheme (Simpson et al. 1993). This scheme has proven to correlate well with the IVL chemical scheme in several comparison studies (Andersson-Sköld and Simpson, 1996). For the EMEP chemical scheme an isoprene emission density of

6 tonnes·km<sup>-2</sup>·year<sup>-1</sup> has also been tested for all VOC/NO<sub>x</sub> emission scenarios.

## 2.7. Simulation scenarios

In order to investigate the transition between high- and low-NO<sub>x</sub> chemistry a whole range of different emission scenarios were compared to make sure that the transition was included. For each of the scenarios, the emissions of NO<sub>x</sub> and VOC were reduced separately and the resulting reduction in ozone concentration was recorded. The results from all scenarios are put together to show which emission reductions that are most effective in which scenarios.

A set of 67 different VOC/NO<sub>x</sub> emission scenarios have been simulated in this study. The scenarios are a theoretical approach to represent the varying conditions within Europe. A trajectory model can only simulate one specific emission scenario at a time and therefore several simulations have been performed to try and describe an area of varying emissions in the same way as a 3D-model would.

For each of the scenarios the emissions of either NO<sub>x</sub> or VOC (including CO) have been reduced by 35 % (Sillman, 1995) and the reduction in ozone and the current values for the indicator species, are noted at 4 p.m. of the simulation since it is during the afternoon that the maximum ozone concentration is obtained. There is thus one reference case as well as one NO<sub>x</sub>-reduced and one VOC-reduced scenario for each of the emission scenarios described in Table 2.4. below. The reductions in ozone from NO<sub>x</sub> and VOC control are calculated as the reference case minus the NO<sub>x</sub> or VOC reduced emission case and the current values for the indicator species are noted from the reference case.

The simulations have started at 1 p.m. and the reduction in ozone has not been noted until 27 hours later. Three different levels of isoprene emissions have also been performed for each set of the 67 emission scenarios which are described in Table 2.4 below.



**Table 2.4.** The emissions of NO<sub>x</sub> and VOC used in the different emission scenarios. The simulations are named after their emissions of NO<sub>x</sub> and VOC. The names start with the letter n (for NO<sub>x</sub> emission) followed by a number which indicates the NO<sub>x</sub> emission level. This number is followed by the letter v (for VOC emission) which is then followed by another number indicating the VOC emission level. The names for the different levels of emissions are the same for both NO<sub>x</sub> and VOC; **level 1= 0.03 tonnes·km<sup>-2</sup>·year<sup>-1</sup>, 2 = 0.1, 3 = 0.3, 4 = 1, 4z = 2, 5 = 3, 5z = 6, 6 = 10, 6z = 20, 7 = 30.**

Name of scenario	NO <sub>x</sub> (tonnes·km <sup>-2</sup> ·year <sup>-1</sup> )	VOC (tonnes·km <sup>-2</sup> ·year <sup>-1</sup> )	VOC/NO <sub>x</sub>	Name of scenario	NO <sub>x</sub> (tonnes·km <sup>-2</sup> ·year <sup>-1</sup> )	VOC (tonnes·km <sup>-2</sup> ·year <sup>-1</sup> )	VOC/NO <sub>x</sub>
n1v1	0.03	0.03	1	n5v3	3	0.3	0.10
n1v2	0.03	0.1	3.3	n5v4	3	1	0.33
n1v3	0.03	0.3	10	n5v4z	3	2	0.67
n1v4	0.03	1	33	n5v5	3	3	1
n1v5	0.03	3	100	n5v5z	3	6	2
n2v1	0.1	0.03	0.30	n5v6	3	10	3.3
n2v2	0.1	0.1	1	n5v6z	3	20	6.7
n2v3	0.1	0.3	3	n5v7	3	30	10
n2v4	0.1	1	10	n5zv4	6	1	0.17
n2v5	0.1	3	30	n5zv4z	6	2	0.33
n2v6	0.1	10	100	n5zv5	6	3	0.50
n3v1	0.3	0.03	0.10	n5zv5z	6	6	1
n3v2	0.3	0.1	0.33	n5zv6	6	10	1.7
n3v3	0.3	0.3	1	n5zv6z	6	20	3.3
n3v4	0.3	1	3.3	n5zv7	6	30	5
n3v5	0.3	3	10	n6v4	10	1	0.10
n3v6	0.3	10	33	n6v4z	10	2	0.20
n3v7	0.3	30	100	n6v5	10	3	0.30
n4v2	1	0.1	0.10	n6v5z	10	6	0.60
n4v3	1	0.3	0.30	n6v6	10	10	1
n4v4	1	1	1	n6v6z	10	20	2
n4v4z	1	2	2	n6v7	10	30	3
n4v5	1	3	3	n6zv4z	20	2	0.10
n4v5z	1	6	6	n6zv5	20	3	0.15
n4v6	1	10	10	n6zv5z	20	6	0.30
n4v6z	1	20	20	n6zv6	20	10	0.50
n4v7	1	30	30	n6zv6z	20	20	1
n4zv4	2	1	0.50	n6zv7	20	30	1.50
n4zv4z	2	2	1	n7v5	30	3	0.10
n4zv5	2	3	1.50	n7v5z	30	6	0.20
n4zv5z	2	6	3	n7v6	30	10	0.33
n4zv6	2	10	5	n7v6z	30	20	0.67
n4zv6z	2	20	10	n7v7	30	30	1
n4zv7	2	30	15				

### 3. Results and discussion

#### 3.1. Total ozone concentration

The maximum ozone concentration varies between the 67 different emission scenarios which have been simulated. All scenarios start with an initial ozone concentration of 70 ppb, but as the emission are released into the box of air along the trajectories, the ozone concentration changes. The simulations using the EMEP chemical scheme have been run for more than four consecutive days while the scenarios using the IVL chemical scheme have been run for two days only. The effect of the different emission scenarios on the ozone concentration is most pronounced at the end of the simulations. The maximum ozone obtained during the last day of simulation, using the EMEP chemical scheme, varies between 20 ppb and 282 ppb for the cleanest and most polluted emission scenario, when no biogenic emission are included (Figure 3.1.)

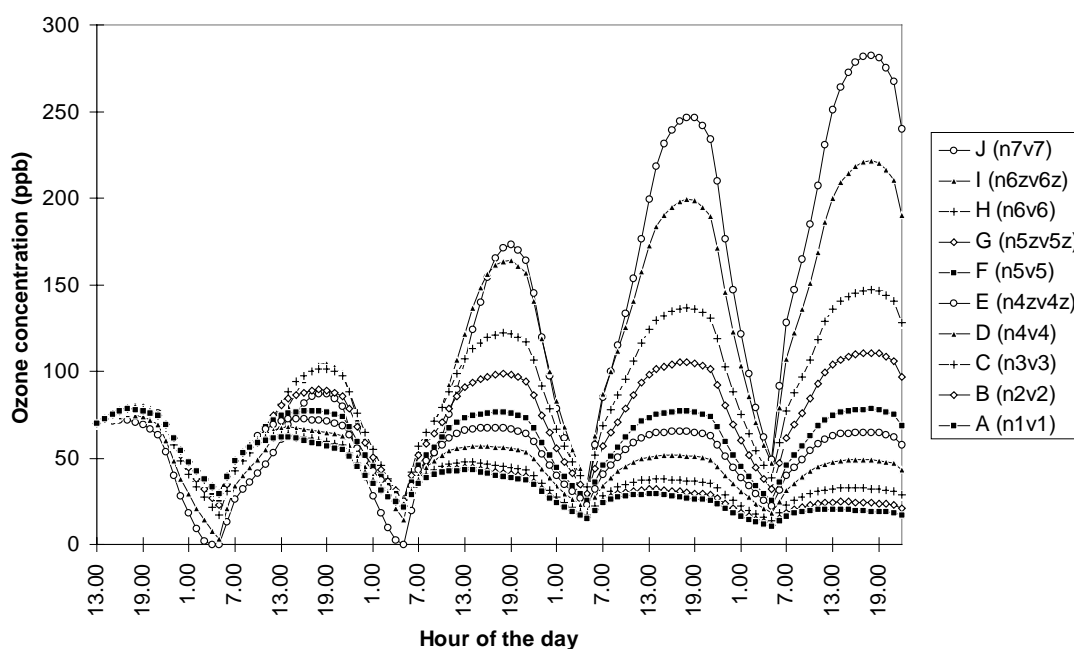


**Figure 3.1.** The ozone concentration in some emission scenarios from simulations using the EMEP chemical scheme. In all scenarios the emissions of  $\text{NO}_x$  and VOC are equal and thus the VOC/ $\text{NO}_x$  ratio is set to unity. There are ten different levels of emission densities; 0.03, 0.1, 0.3, 1, 2, 3, 6, 10, 20 and 30 tonnes·km<sup>-2</sup>·year<sup>-1</sup> named A, B, ..., J, where emission scenario A is least polluted and emission scenario J is most polluted. The names within brackets refer to the names in Table 2.4. No isoprene emissions have been included.

When the results from the simulations using the IVL chemical scheme are compared with the results from the simulations using the EMEP chemical scheme, there are

differences in the calculated ozone concentrations. The conditions for the simulations are identical, thus the differences is explained by the use of different chemical schemes. It is in the most polluted scenarios which this is most clearly seen (Figure 3.2.). In the two most severely polluted scenarios, the  $\text{NO}_x$  emissions are so high that a large part of the ozone, is directly titrated to  $\text{NO}_2$  through the reaction with NO (reaction 3). Since  $\text{NO}_x$  has a shorter atmospheric lifetime than most VOC, the chemical composition changes as more emissions are released into the plume. When the plumes continue, more VOC is built up, and the formation of ozone takes off since peroxy radicals are formed from VOC and compete with ozone for reaction with NO. This reduces the reaction between NO and ozone and thus the ozone concentration increases. In the simulations using the IVL chemical scheme it takes longer for the ozone concentration to recover from the titration caused by the high NO concentrations. The recovery process depends on the chemical description of the VOC decomposition, which is described in different ways in the chemical schemes.

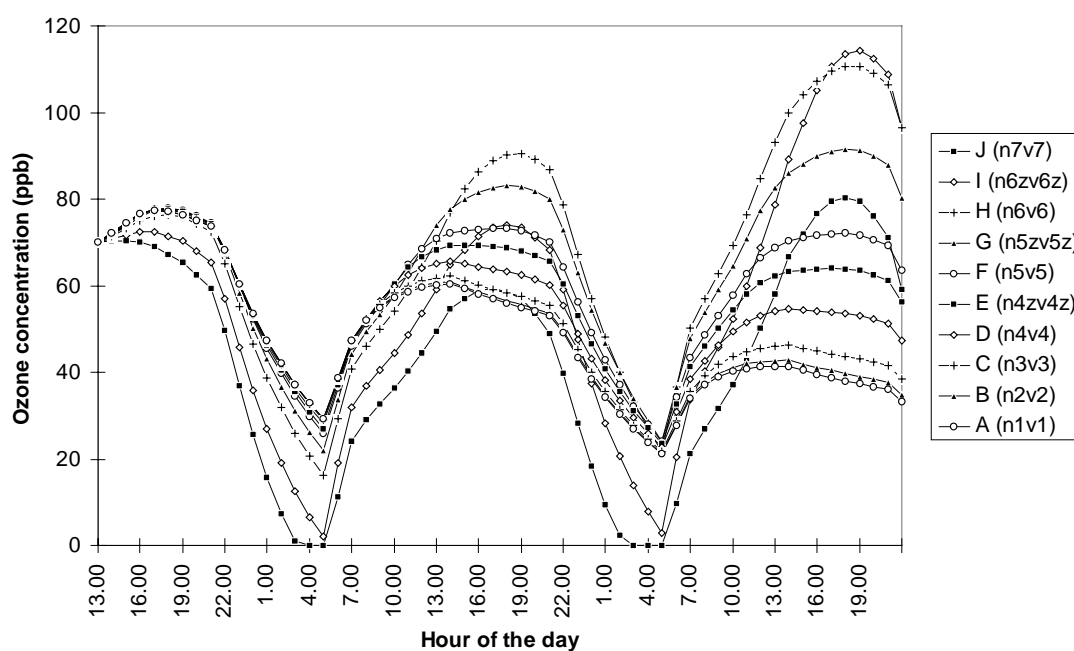


**Figure 3.2.** The ozone concentration in some emission scenarios from simulations using the IVL chemical scheme. In all scenarios the emissions of  $\text{NO}_x$  and VOC are equal and thus the VOC/ $\text{NO}_x$  ratio is set to unity. There are ten different levels of emission densities; 0.03, 0.1, 0.3, 1, 2, 3, 6, 10, 20 and 30 tonnes·km<sup>-2</sup>·year<sup>-1</sup> named A, B, ..., J, where emission scenario A is least polluted and emission scenario J is most polluted. The names within brackets refer to the names in Table 2.4. No isoprene emissions have been included.

When isoprene emissions are included, the maximum ozone increases with a few ppb in the least polluted emission scenario, using the EMEP chemical scheme. In the most polluted environment, the maximum ozone concentration increases with 29 ppb and

reaches 311 ppb when isoprene emissions of  $6 \text{ tonnes}\cdot\text{km}^{-2}\cdot\text{year}^{-1}$  is included. The absolute emission density of the isoprene emissions are the same in all scenarios, which means that in the least polluted scenarios, the isoprene emissions are much higher than the total emissions of other VOC. In the highly polluted scenarios, the emissions of isoprene are relatively much lower than the emissions of other VOC, but still the effect on the ozone concentration is much larger in these scenarios. This reflects the  $\text{NO}_x$  limitation of the clean scenarios and shows that additional VOC emissions have little or no impact on the ozone concentration in these scenarios. In the highly polluted scenarios there are enough  $\text{NO}_x$  to make use of the additional isoprene emissions and thus more ozone is produced due to these added emissions. Figure 3.3. shows the ozone concentration in a scenario C (n3v3) and J (n7v7) from Figure 3.1., both without isoprene emissions and with isoprene emissions of  $3 \text{ tonnes}\cdot\text{km}^{-2}\cdot\text{year}^{-1}$ .

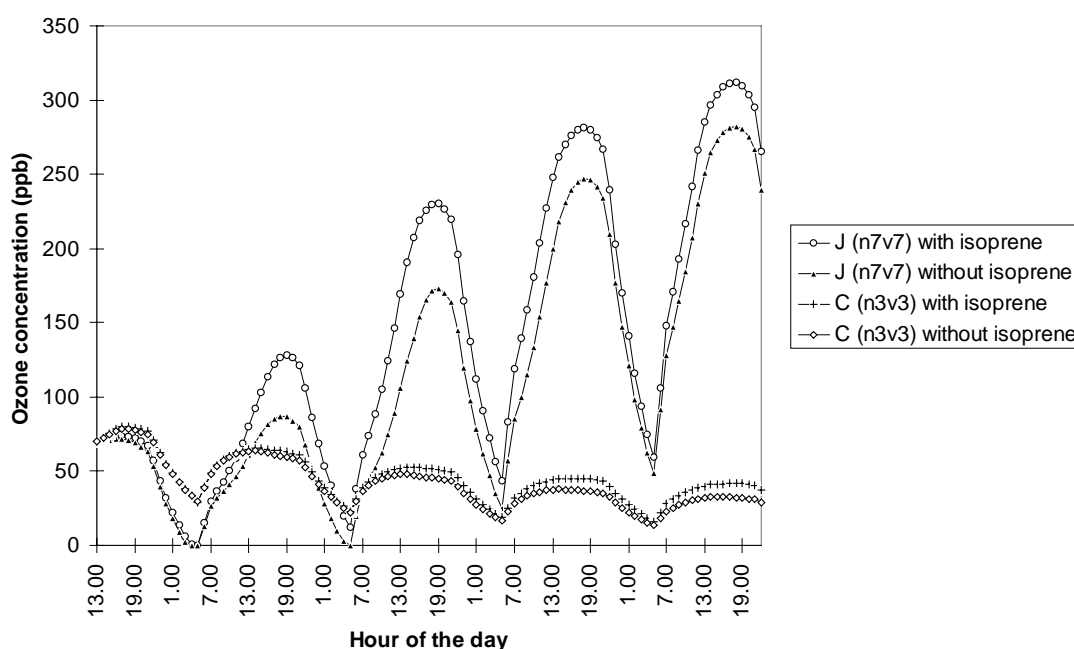


**Figure 3.3.** The ozone concentration in the rather clean scenario C (n3v3) and in the highly polluted scenario J (n7v7), both without any isoprene emissions and with isoprene emissions of  $3 \text{ tonnes}\cdot\text{km}^{-2}\cdot\text{year}^{-1}$ , in simulations using the EMEP chemical scheme. In scenario A the emissions of  $\text{NO}_x$  and VOC are both set to  $0.03 \text{ tonnes}\cdot\text{km}^{-2}\cdot\text{year}^{-1}$  and in scenario J the emissions of  $\text{NO}_x$  and VOC are set to  $30 \text{ tonnes}\cdot\text{km}^{-2}\cdot\text{year}^{-1}$ . The names within brackets refer to the names in Table 2.4.

The emissions of CO have been varied along with the VOC emissions in each scenario while the background emissions of  $\text{CH}_4$  has been set to a constant level in all scenarios. The CO emissions have been set to 3.7 times the VOC emissions but simulations using CO emissions set to a factor of 2 or 5 times the VOC emissions have also been performed. The emissions of  $\text{CH}_4$ , which are normally set to a certain constant value, have been excluded in some simulations. These tests with varying

emissions of CH<sub>4</sub> and CO show the same results as for isoprene, the ozone concentration increases more in the high NO<sub>x</sub> scenarios than in the low NO<sub>x</sub> scenarios.

### **3.2. Changes in ozone due to emission reductions**

In all of the 67 different emission scenarios, 35 % reductions of either the NO<sub>x</sub> or the VOC and CO emissions have been performed and the effects on the ozone concentrations have been studied (Sillman, 1995). The CO emissions have also been reduced along with the VOC emissions since they are initially varied according to the VOC emissions.

#### ***3.2.1. Average changes in ozone***

The change in ozone due to an emission reduction has been recorded both as the average change in ozone during some hours and as the absolute change in the concentration during the afternoon, when the ozone concentration reaches its maximum diurnal concentration.

The emission reductions are performed during the entire trajectories and the changes in ozone are thus more noticeable at the end of the simulations. Due to this the largest change in ozone, from a reduction of VOC and CO emissions, is seen as the change in the afternoon ozone concentration on the last day of the simulation. The average change in ozone, calculated from the start of the simulation, is lower than any of the afternoon values. For the NO<sub>x</sub> emission reductions, the behaviour is the same as for a VOC and CO emissions reduction, for those scenarios which are NO<sub>x</sub> limited. Also in the scenarios where NO<sub>x</sub> emission reductions give a higher ozone concentration than without emission reductions, the average change in ozone is less than the afternoon changes in ozone. The only difference is that in these highly polluted scenarios, the change in ozone is negative and becomes more and more negative at the end of the simulations. In the scenarios which are in the transition area between NO<sub>x</sub> limited scenarios and VOC limited scenarios, the first response to a NO<sub>x</sub> emission reduction is an increase in the ozone while it later in the simulation gives a lower ozone concentration.

The changes in ozone follows the same pattern regardless of whether average changes or changes in maximum ozone is analysed.

### 3.2.2. Changes in maximum ozone concentration

As explained in the section above, the changes in ozone, due to emission reductions along the entire trajectories, are largest during the last day of the simulation. In Figure 3.4. below the changes in ozone per tonnes·km<sup>-2</sup>·year<sup>-1</sup> emission reduction, at 4 p.m. at day two of the simulation, due to emission reductions of either NO<sub>x</sub> or VOC and CO by 35 %, are given. The scenarios are sorted according to NO<sub>x</sub> emissions which increase along the x-axis. The VOC emissions also increase along the x-axis but only within each individual level of NO<sub>x</sub> emissions. The least polluted scenarios have been left out so that only 40 out of the total 67 emission scenarios are given in Figure 3.4. The cleaner scenarios which are not given in Figure 3.4., shows the same behaviour as the scenarios to the left in the figure but with larger changes in ozone due to NO<sub>x</sub> emission reductions and smaller changes in ozone due to reductions of VOC and CO emissions.

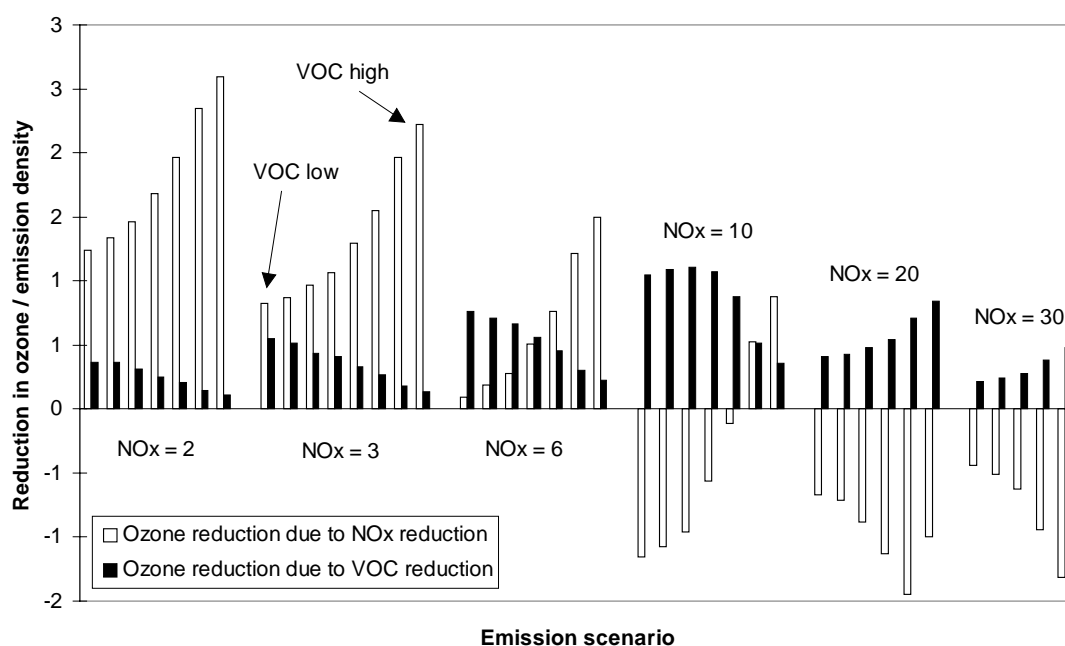


**Figure 3.4.** The change in ozone concentration per emission reduction in tonnes·km<sup>-2</sup>·year<sup>-1</sup>, at 4 p.m. on the day after the start of the simulations, using the IVL chemical scheme. The white bars give the change in ozone from a NO<sub>x</sub> reduction and the black bars show the change due to an emission reduction of VOC and CO. No isoprene emissions have been included. The scenarios are sorted primarily by the NO<sub>x</sub> emissions, which are noted in the figure in tonnes·km<sup>-2</sup>·year<sup>-1</sup>, and secondarily by the VOC emissions. The scenarios with low VOC are to the left, and the scenarios with high VOC are to the right, within each individual NO<sub>x</sub> level which is indicated in the figure for the scenarios with NO<sub>x</sub> = 3 tonnes·km<sup>-2</sup>·year<sup>-1</sup> as an example.

The absolute availability of NO<sub>x</sub> controls the ozone formation to a large extent. The effect on the ozone concentration due to a NO<sub>x</sub> emission reduction, calculated per

reduced tonnes·km<sup>-2</sup>·year<sup>-1</sup> of NO<sub>x</sub>, is higher at low levels of NO<sub>x</sub>, where NO<sub>x</sub> limits the ozone production. Within each level of NO<sub>x</sub> emissions, the ozone formation varies due to the availability of VOC. The reduction in ozone, calculated per reduced tonnes·km<sup>-2</sup>·year<sup>-1</sup> of NO<sub>x</sub>, is higher when the VOC emissions, and thus the VOC/NO<sub>x</sub> ratio, are higher. Not until at a certain level of NO<sub>x</sub> emissions, is there a change from NO<sub>x</sub> sensitivity to VOC sensitivity, i.e. that the change in ozone is larger for a VOC emission reduction than for a NO<sub>x</sub> emission reduction. The transition takes place at a NO<sub>x</sub> emission density of around 6 to 10 tonnes·km<sup>-2</sup>·year<sup>-1</sup>, and a VOC/NO<sub>x</sub> ratio of around 1 or 2. Below this level of NO<sub>x</sub> emissions, the change in ozone is larger for a NO<sub>x</sub> emission reduction regardless of the VOC emission density, despite the fact that this includes scenarios with a VOC/NO<sub>x</sub> ratio in between 0.01 and 100. Above this level of NO<sub>x</sub> emissions, the scenarios are VOC sensitive and reductions of the NO<sub>x</sub> emissions lead to an increase in the ozone concentration.

The change in ozone due to a reduction of the VOC and CO emissions is more affected by the absolute NO<sub>x</sub> emissions than by the VOC emissions in the background. The change in ozone from a VOC and CO emission reduction is largest, calculated per reduced tonnes·km<sup>-2</sup>·year<sup>-1</sup> of VOC, in those scenarios where the change from NO<sub>x</sub> to VOC limited chemistry takes place. Within each individual level of NO<sub>x</sub> emissions in the NO<sub>x</sub> limited scenarios, the change in ozone, due to a VOC and CO emission reduction, is larger in those scenarios where the VOC emissions are low, i.e. when the VOC/NO<sub>x</sub> ratio is low. In the VOC sensitive scenarios the relation is the opposite. Within each level of NO<sub>x</sub> emissions, the change in ozone, due to a reduction of VOC and CO emissions calculated per reduced tonnes·km<sup>-2</sup>·year<sup>-1</sup> of VOC, is instead larger when the VOC emissions are larger.

Apart from the fact that NO<sub>x</sub> emission reductions cause an increase in the ozone concentration in some scenarios, the absolute changes in the ozone concentrations is always larger for NO<sub>x</sub> reductions than for reductions in VOC and CO.

As explained above, the NO<sub>x</sub> background emissions controls the impact of emission reductions to a larger extent than the VOC background emissions. This is seen in Figure 3.4. above where the emission scenarios are sorted primarily by the NO<sub>x</sub> emissions and secondarily by the VOC emissions. A change over from NO<sub>x</sub> to VOC sensitivity takes place first at a certain NO<sub>x</sub> level. In Figure 3.5. below the same data as in Figure 3.4. is shown, but with the scenarios in a different order. In Figure 3.5. the scenarios are sorted primarily by their VOC background emissions and secondarily by their NO<sub>x</sub> background emissions, instead of the other way around. There is a change

over from  $\text{NO}_x$  to VOC sensitivity for each individual level of background VOC emissions as the  $\text{NO}_x$  emissions increase, which is clearly seen in Figure 3.5.

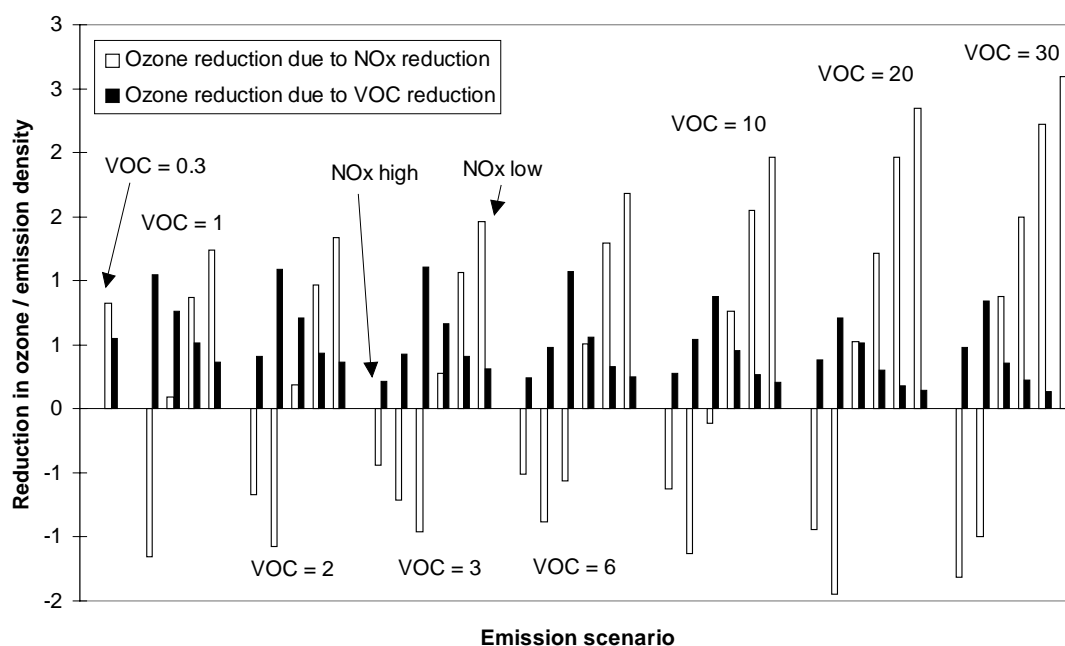


**Figure 3.5.** The change in ozone concentration per emission reduction in  $\text{tonnes}\cdot\text{km}^{-2}\cdot\text{year}^{-1}$ , at 4 p.m. on the day after the start of the simulations, using the IVL chemical scheme. The white bars give the change in ozone from a  $\text{NO}_x$  reduction and the black bars show the change due to an emission reduction of VOC and CO. No isoprene emissions have been included. The scenarios are sorted primarily by the VOC emissions, which are noted in the figure in  $\text{tonnes}\cdot\text{km}^{-2}\cdot\text{year}^{-1}$ , and secondarily by the  $\text{NO}_x$  emissions. The scenarios with high  $\text{NO}_x$  are to the left, and the scenarios with low  $\text{NO}_x$  are to the right, within each individual VOC level which is indicated in the figure for the scenarios with VOC = 3  $\text{tonnes}\cdot\text{km}^{-2}\cdot\text{year}^{-1}$  as an example.

The net effect on the ozone concentration, when reducing both  $\text{NO}_x$  and VOC emissions at the same time, is not necessarily equal to the sum of the individual changes in ozone, caused by either of the emission reductions. The effect may be both less or more than additive and depends on whether maximum or average changes in ozone are compared. Simulations have been performed where the emission of  $\text{NO}_x$ , VOC and CO were reduced by 35 % at the same time. This did not give the same result as the calculated net effect from the changes in ozone caused by individual emission reductions of the different species. In Figure 3.6. below, the actual effect from a change in  $\text{NO}_x$ , VOC and CO at the same time and the calculated net effect from the individual emission changes, are compared. The scenarios are sorted primarily by the  $\text{NO}_x$  emissions and secondarily by the VOC emissions, exactly as in Figure 3.4.



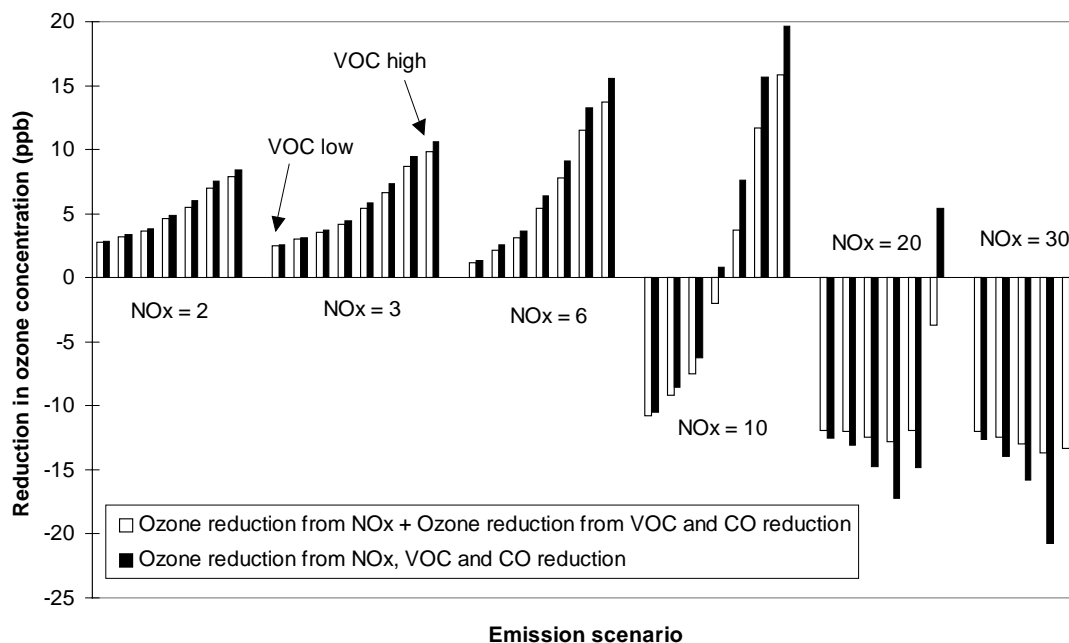


**Figure 3.6.** The change in ozone concentration per emission reduction in tonnes·km<sup>-2</sup>·year<sup>-1</sup>, at 4 p.m. on the day after the start of the simulations, using the IVL chemical scheme. The black bars give the change in ozone from a reduction of NO<sub>x</sub>, VOC and CO at the same time. The white bars show the calculated net change in ozone from the individual emission changes in NO<sub>x</sub> and VOC & CO. No isoprene emissions have been included. The names of the scenarios refer to the notation used in Table 2.4.

### 3.2.3. Changes in ozone from emission reductions, with biogenic emissions present

When biogenic emissions are included in the simulations, this changes the VOC/NO<sub>x</sub> ratio of the scenarios. The changes in ozone due to NO<sub>x</sub> emission reductions are larger when biogenic emissions are included, while the changes in ozone due to reduced anthropogenic VOC emissions are smaller than without biogenic emissions. The VOC emission reduction causes a lower change in ozone since there are biogenic VOC available for reaction. The absolute change in VOC is the same as in the scenarios without biogenic emission, but the relative change in VOC is smaller and thus the change in ozone becomes lower. The change in ozone is higher for a NO<sub>x</sub> emission reduction because there are more total VOC available for reaction when biogenic emission are included. Since the ozone production is higher when biogenic emissions are available, a NO<sub>x</sub> emissions reduction will reduce a larger absolute amount of ozone when biogenic emissions are present. The change over from NO<sub>x</sub> sensitivity to VOC sensitivity still takes place at the same level of NO<sub>x</sub> emissions, but at a slightly

lower ratio between anthropogenic VOC and NO<sub>x</sub>, since there are biogenic VOC around to make the total VOC/NO<sub>x</sub> ratio higher.

### **3.3. Indicator species**

The indicator species which were set up in Sillman (1995) and evaluated for US conditions (see Table 1.1.) have been calculated using a trajectory model approach.

The concentrations of many species in the atmosphere show a distinct diurnal variation due to the diurnal variation in photochemical activity. The indicator species are therefore very sensitive to the hour of the day for which they are studied. In a 3D model, each individual grid square, i.e. the air mass in the grid square, is followed separately. The air flows in and out of the different grid squares and the same air mass is therefore not contained within the same grid cell, but flows with the direction of the wind to other grid cells in the model. For each moment in time, the air mass in a certain grid square can thus be described as the air in a trajectory which arrives at that grid square at that specific time. For each hour of the day there is data available from each individual grid cell which can be regarded as data from an equally large number of trajectories. In a trajectory model however, only one specific trajectory or emission scenario may be simulated at a time, and therefore several simulations have to be performed to get the same data set as from a 3D-model.

The indicator species have been recorded at 4 p.m., since the maximum ozone concentration is reached during the afternoon. In Sillman (1995) the indicators were calculated at maximum ozone. The hour of the day for the maximum ozone concentration varies between the emission scenarios from 2 p.m. to 6 p.m. and therefore the average hour (4 p.m.) has been used in all scenarios to make sure that the results are not affected by differences in the meteorological conditions.

The simulations start at 1 p.m. and the indicator species which are evaluated below are based on the values from the afternoon on the day after the start of the simulations (i.e. 27 hours after the start of the simulation)

#### **3.3.1. *The indicator species NO<sub>y</sub>***

The total reactive nitrogen NO<sub>y</sub> = NO + NO<sub>2</sub> + HNO<sub>3</sub> + PAN + PAN analogues + organic nitrates is, as the name suggests, a measure of the total available nitrogen in

the atmosphere. This parameter has, for studies in eastern USA shown a correlation to the ozone sensitivity toward changes in  $\text{NO}_x$  and VOC emissions. In Figure 3.7., the changes in ozone due to emission reductions of either  $\text{NO}_x$  or VOC and CO are plotted versus  $\text{NO}_y$  at 4 p.m.

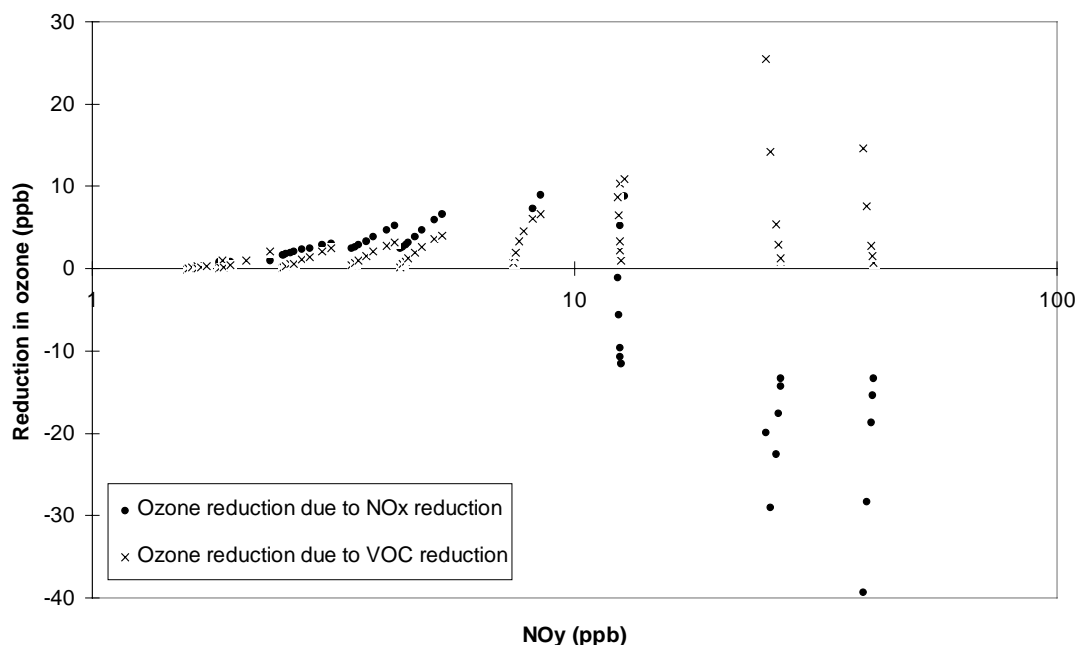


**Figure 3.7.** The change in ozone concentration, due to emission reductions of  $\text{NO}_x$  or VOC and CO, versus  $\text{NO}_y$ , at 4 p.m. on the day after the start of the simulations. The IVL chemical scheme has been used in the simulations. No isoprene emissions have been included. Note that the scale on the x-axis is logarithmic.

The data points in Figure 3.7. are collected in several groups in the graph. Each group of data points originate from simulations having identical  $\text{NO}_x$  emissions. The simulations which experience low  $\text{NO}_x$  emissions also show low  $\text{NO}_y$  values and are to the left of the graph. For the groups of data at low  $\text{NO}_y$  concentration, the scenarios are  $\text{NO}_x$  limited which can be seen since the reduction in ozone from a  $\text{NO}_x$  emission reduction is larger than for a VOC emission reduction. Within each group representing a certain  $\text{NO}_x$  background emission level, there is a positive slope for the  $\text{NO}_x$  limited scenarios. The smallest and the largest reductions in ozone within each group of data originate from the simulations with lowest and highest VOC emissions. The reduction in ozone, due to a point source of  $\text{NO}_x$ , is thus largest in the scenario which experience largest VOC emissions within each individual level of  $\text{NO}_x$  emissions. This was also shown previously in Figure 3.4. The reduction in ozone due to a reduction of the VOC emission does not behave in the same way as for a  $\text{NO}_x$  emission reduction, even though it may seem so from Figure 3.7. The absolute reduction in VOC emissions varies between the data points within each group of data

in Figure 3.7. and thus the largest change in ozone originates from a much larger VOC emission reduction.

The change from  $\text{NO}_x$  sensitivity to VOC sensitivity seem to take place at the two sets of data which are at 8 and 12 ppb of  $\text{NO}_y$ . These data points originate from simulations with  $\text{NO}_x$  emission densities of 6 and 10 tonnes·km<sup>-2</sup>·year<sup>-1</sup>. This was previously shown in Figure 3.4.

The two remaining groups of data at around 25 and 40 ppb  $\text{NO}_y$ , are VOC sensitive and the reduction of VOC give large changes in ozone while the reduction of  $\text{NO}_x$  emission actually increase the ozone concentration (shown as a negative reduction in Figure 3.7.).

The overall look of Figure 3.7. is similar to the results in Sillman (1995). The absolute changes in ozone are smaller in this study which is explained by the lower total ozone concentrations. In Sillman (1995), an episode with ozone concentrations higher than 150 ppb was simulated. The appearance of individual groups of data points in the graph is a result from the rather theoretical construction of emissions scenarios at different emission levels. In a 3D model the emissions in the different scenarios are not divided into separate levels, but are instead more spread out.

### **3.3.2. *The indicator species $\text{O}_3/(\text{NO}_y-\text{NO}_x)$***

The species  $\text{O}_3/(\text{NO}_y-\text{NO}_x)$  can be seen as the amount of ozone which have been produced per oxidised nitrogen in the atmosphere. The changes in ozone due to emission reductions of either  $\text{NO}_x$  or VOC and CO are plotted versus  $\text{O}_3/(\text{NO}_y-\text{NO}_x)$  at 4 p.m. in Figure 3.8. below.

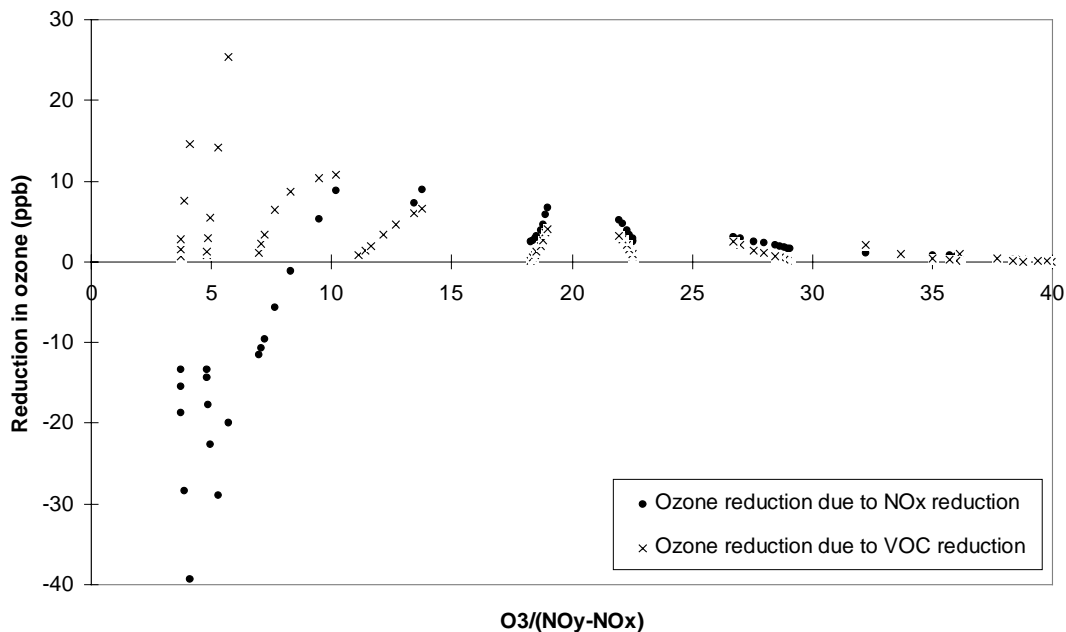


**Figure 3.8.** The change in ozone concentration, due to emission reductions of  $\text{NO}_x$  or VOC and CO, versus  $\text{O}_3/(\text{NO}_y-\text{NO}_x)$ , at 4 p.m. on the day after the start of the simulations. The IVL chemical scheme has been used in the simulations. No isoprene emissions have been included.

Exactly as in Figure 3.7., the data points in this graph are collected in groups. The data points in each group are all from simulations with the same level of  $\text{NO}_x$  emissions. The data points from scenarios with low  $\text{NO}_x$  emissions all have high  $\text{O}_3/(\text{NO}_y-\text{NO}_x)$  values. These cases are  $\text{NO}_x$  limited, thus  $\text{NO}_x$  emissions produce more ozone per molecule than in the VOC limited scenarios which are at the low end of the x-axis. From this graph the change over from  $\text{NO}_x$  to VOC sensitivity seem to happen for the group of data with  $\text{O}_3/(\text{NO}_y-\text{NO}_x)$  in between 11 and 14 which all have a  $\text{NO}_x$  emission density of  $6 \text{ tonnes}\cdot\text{km}^{-2}\cdot\text{year}^{-1}$ .

Despite the fact that there are much fewer data points to analyse from this trajectory model study than there are from a 3D model study, Figure 3.8. still shows about the same overall results as in Sillman (1995)

### 3.3.3. The indicator species $\text{HCHO}/\text{NO}_y$

Almost all VOC form HCHO at some stage of their degradation pathway in the atmosphere, and therefore the species  $\text{HCHO}/\text{NO}_y$  gives a relation between the amount of oxidised VOC and the total available nitrogen of the atmosphere. The

relation between the changes in ozone due to emission reductions of  $\text{NO}_x$  or VOC and CO, and the  $\text{HCHO}/\text{NO}_y$  ratio is given in Figure 3.9.

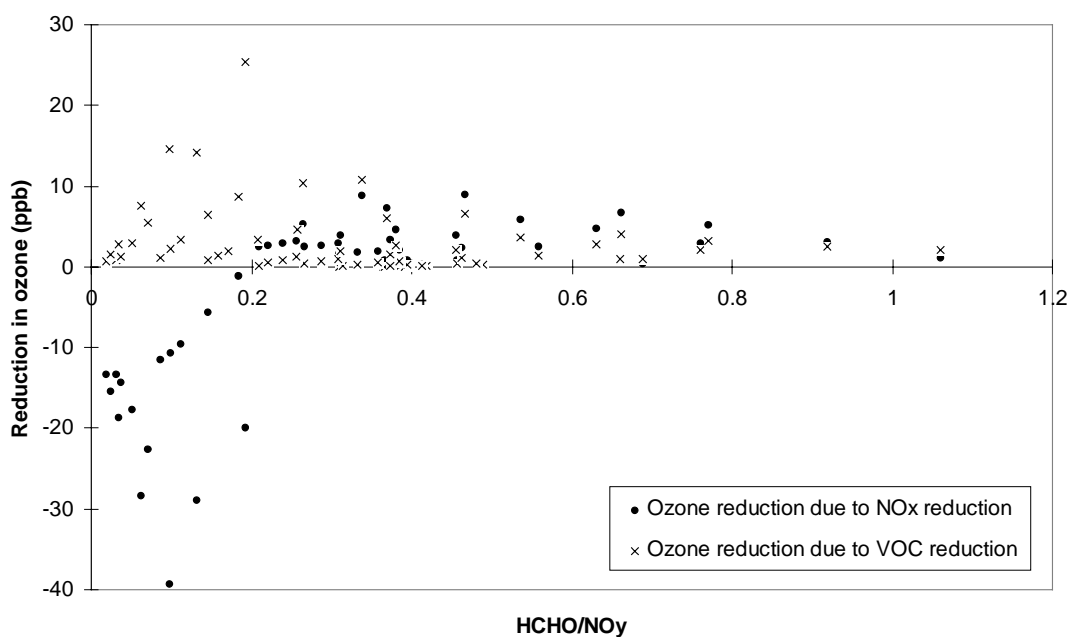


**Figure 3.9.** The change in ozone concentration, due to emission reductions of  $\text{NO}_x$  or VOC and CO, versus  $\text{HCHO}/\text{NO}_y$ , at 4 p.m. on the day after the start of the simulations. The IVL chemical scheme has been used in the simulations. No isoprene emissions have been included.

In Figure 3.9., no groups of data points can be distinguished as in Figure 3.7. and 3.8. There is not such a clear distinction between the  $\text{NO}_x$  and VOC sensitive scenarios in this graph either. According to Sillman (1997) this indicator species did not work as well as the other, and it was not consistent in the different model scenarios which were tested.

### 3.3.4. *The indicator species $\text{H}_2\text{O}_2/\text{HNO}_3$*

The  $\text{H}_2\text{O}_2/\text{HNO}_3$  ratio directly compares the relative importance of the different termination reactions for odd hydrogen (reactions 5 - 7). In Figure 3.10., the change in ozone due to emission reductions of either  $\text{NO}_x$  or VOC and CO versus the  $\text{H}_2\text{O}_2/\text{HNO}_3$  ratio is given.

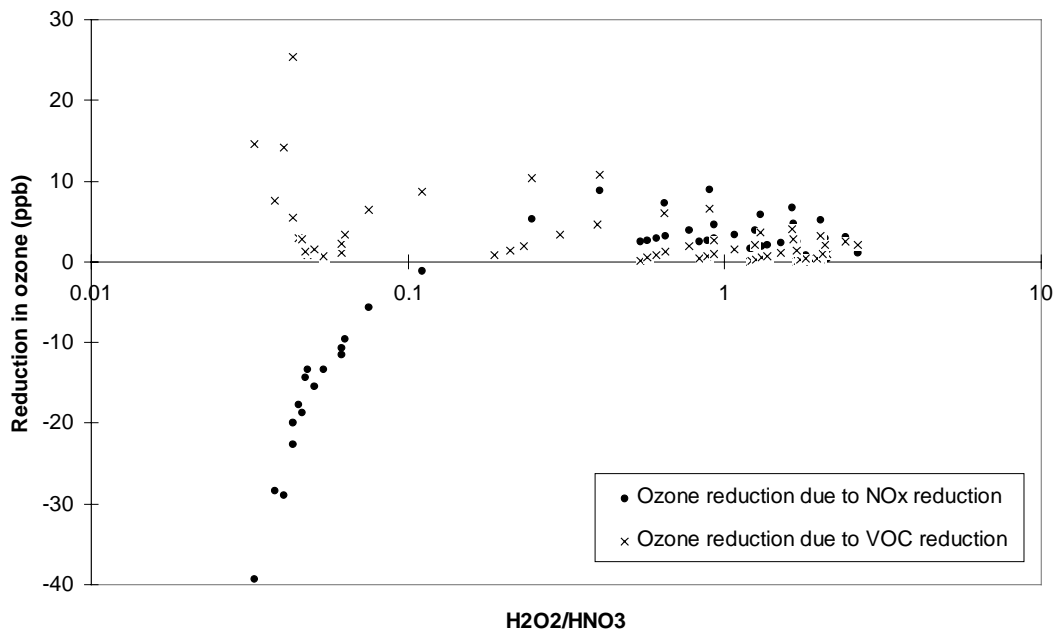


**Figure 3.10.** The change in ozone concentration, due to emission reductions of  $\text{NO}_x$  or VOC and CO, versus  $\text{H}_2\text{O}_2/\text{HNO}_3$ , at 4 p.m. on the day after the start of the simulations. The IVL chemical scheme has been used in the simulations. No isoprene emissions have been included. Note that the scale on the x-axis is logarithmic.

In Figure 3.10., the VOC sensitive area is distinguished where the  $\text{H}_2\text{O}_2/\text{HNO}_3$  ratio is low. These data points are derived from the emission scenarios with high  $\text{NO}_x$  emissions. For the higher  $\text{H}_2\text{O}_2/\text{HNO}_3$  ratios, the data points are more spread out but there is still a  $\text{NO}_x$  sensitivity to be seen, despite the spread in data. In Sillman (1995) this indicator was the indicator which showed the most distinct transition of all the indicators and it also showed consistency in the different model scenarios. This distinct transition is not seen in this study for this indicator.

### 3.3.5. Values for indicator species on different days along a trajectory

When the indicator species are studied at a later day along the same trajectory the plume will have built up in VOC and the VOC/ $\text{NO}_x$  ratio has therefore increased compared to the start of the trajectory. The overall look of the graphs of the indicator species do not change despite the fact that the absolute values of both the changes in ozone as well as the values of the indicator species increase and are more spread out. The transition values do not change except for  $\text{NO}_y$  which seem to increase slightly with time.

### ***3.3.6. Values for indicator species when biogenic emissions are present***

When biogenic emissions are included in the simulations, there is a larger difference in the change of ozone caused by a NO<sub>x</sub> emission reduction compared to the change in ozone caused by a VOC emission reduction. This makes it easier to separate the NO<sub>x</sub> and VOC sensitive areas in the graphs of the indicator species. The transition values are slightly affected by the presence of biogenic VOC. The transition value for O<sub>3</sub>/(NO<sub>y</sub>-NO<sub>x</sub>) decreases slightly while the other indicator species increase. The overall appearance of the graphs of indicator species however, do not change.



## 4. Conclusions

In Sillman (1995) the areas of NO<sub>x</sub> and VOC sensitivity was determined from a much larger data set than what have been produced in this study. A data point was said to be NO<sub>x</sub> sensitive if a 35 % NO<sub>x</sub> reduction caused a reduction in ozone, which exceeded the reduction in ozone caused by a 35 % reduction in VOC, by 5 ppb or more. This definition is difficult to translate directly to the study performed here since the total ozone was on an average much higher in the study performed by Sillman (1995). For the indicator species NO<sub>y</sub> and O<sub>3</sub>/(NO<sub>y</sub>-NO<sub>x</sub>) there are not a full range of values since the data points are collected together in small groups of data which makes it difficult to determine the value for which the transition occurs. Due to the relatively rather small data set the transition values between NO<sub>x</sub> and VOC sensitivity have only been estimated directly from the graphs and are given in Table 4.1. below.

**Table 4.1.** Transition values for the indicator species defined in Sillman (1995) for the transition between NO<sub>x</sub> and VOC sensitivity under European conditions without any isoprene emissions using the IVL chemical scheme.

Indicator species	NO <sub>x</sub> sensitive	VOC sensitive
NO <sub>y</sub>	< 8-12 ppb	> 8-12 ppb
O <sub>3</sub> /(NO <sub>y</sub> - NO <sub>x</sub> )	> 11-13	< 11-13
HCHO/NO <sub>y</sub>	> 0.2	< 0.2
H <sub>2</sub> O <sub>2</sub> /HNO <sub>3</sub>	> 0.3	< 0.3

When biogenic emissions are included in the simulations, the transition values of NO<sub>y</sub>, HCHO/NO<sub>y</sub> and H<sub>2</sub>O<sub>2</sub>/HNO<sub>3</sub> increased slightly while the transition value for O<sub>3</sub>/(NO<sub>y</sub> - NO<sub>x</sub>) decreases slightly. Biogenic VOC emission were included in the study by Sillman (1995) and should also be included since they are a part of the natural atmosphere. The transition values are however fairly consistent in the different model scenarios regarding biogenic emissions. This is also true when the indicator species are compared between for different days along the same trajectories. Regardless of which day that is considered the transition values stays the same except for NO<sub>y</sub> which increases slightly.

One difference between this study and the study by Sillman (1995), is that the 35 % reduction in VOC emissions have always been accompanied with a 35 % reduction of the CO emissions in this study. In Sillman (1995) the change in ozone from VOC emission reductions in NO<sub>x</sub> sensitive areas are close to zero which is not seen in this

study. When both VOC and CO is reduced, as in this study, the total emission reduction is larger and thus the reductions in ozone become larger.

This study has shown that it is possible to use the concept of indicator species in a trajectory model. The results are reasonably consistent with the findings in Sillman (1995) but further studies are needed in order to determine the actual transition values suitable for European conditions.

## **5. Acknowledgements**

The author wish to thank Dr Sanford Sillman at the Department of Atmospheric, Oceanic, and Space Sciences, University of Michigan in Ann Arbor, USA, for his help with, and comments on, the model set-up as well as helpful suggestions regarding the results. The discussions regarding the results and many suggestions concerning the report, from Karin Pleijel at the Swedish Environmental Research Institute (IVL) in Göteborg, Sweden, are highly appreciated.

This project has been funded by the Swedish Environmental Protection Agency which are gratefully acknowledged.

## 6. References

- AEA Technology (1995) FACSIMILE v 4.0 User guide, AEA Technology, Harwell, Didcot, Oxfordshire OX11 0RA, United Kingdom.
- Altenstedt, J. and Andersson-Sköld, Y. (1995) Sensitivity studies of the chemical scheme of the IVL photochemical trajectory model, Swedish Environmental Research Institute (IVL) Report B-1217, Göteborg, Sweden.
- Altshuler S.L., Arcadio T.D. and Lawson D.R. (1995) Weekday vs. Weekend Ambient Ozone Concentrations: Discussion and Hypothesis with Focus on Northern California, *J. Air & Waste Manage. Assoc.*, **45**, pp 967-972.
- Andersson-Sköld, Y. (1995) Updating the chemical scheme for the IVL photochemical trajectory model, Swedish Environmental Research Institute (IVL) Report B-1151, Göteborg, Sweden.
- Andersson-Sköld, Y., Grennfelt, P. and Pleijel, K. (1992) Photochemical ozone creation potentials - a study of different concepts. *J. Air Waste Manage. Assoc.*, **42**, No. 9, pp 1153-1158.
- Andersson-Sköld Y. and Simpson D. (1996) Comparison of the chemical schemes of the EMEP MSC-W and the IVL photochemical trajectory models, poster presented at the EUROTRAC Symposium on Transport and Transformation of Pollutants in the Troposphere, Garmisch-Partenkirchen, March 25-29, 1996.
- Bowman F.M. and Seinfeld J.H. (1994) Ozone productivity of atmospheric organics, *J. Geophys. Res.*, **99**, No. D3, pp 5309-5324
- Chameides, W.L., Fehsenfeld, F., Rodgers, M.O., Cardeling, C., Martinez, J., Parrish, D., Lonneman, W., Lawson, D.R., Rasmussen, R.A., Zimmerman, P., Greenberg, J., Middleton, P. and Wang, T. (1992) Ozone Precursor Relationships in the Ambient Atmosphere. *J. Geophys. Res.*, **97**, No. D5, 6037-6055.
- Derwent, R.G. and Hov, Ø. (1979) Computer modelling studies of photochemical air pollution in North West Europe. AERE R-9434, Harwell Laboratory, Oxfordshire, England.
- Derwent, R.G. and Hough, A.M., (1988) The impact of possible future emission control regulations on photochemical ozone formation in Europe, AERE R-12919, Harwell Laboratory, Oxfordshire, England.
- Gear, C. W. (1969) The automatic integration of stiff ordinary differential equations. *Information Processing 68*, Ed. A. J. H. Morell, North Holland, Amsterdam, 1969, pp. 187-193.

- Janhäll, S., Altenstedt, J., Andersson-Sköld, Y. and Lindskog, A. (1995) Regionala emissioners inverkan på de marknära ozonhalterna i södra Sverige, Swedish Environmental Research Institute (IVL) Report B-1202 (in Swedish), Göteborg, Sweden.
- Janhäll, S. and Andersson-Sköld, Y. (1997) Emission inventory on NMVOC species in Sweden, Swedish Environmental Institute (IVL) Report B-1163, Göteborg, Sweden.
- Kuhn, M., Builtjes, P., Poppe, D., Simpson, D., Stockwell, W.R., Andersson-Sköld, Y., Baart, A., Das, M., Fiedler, F., Hov, Ø., Kirchner, F., Makar, P.A., Milford, J.B., Roemer, M., Ruhnke, R., Strand, A., Vogel, B. and Vogel H. (1998) Intercomparison of the gas-phase chemistry in several chemistry and transport models, *Atmos. Environ.*, **32**, No 4, 693-709).
- Lin X., Trainer M. and Liu S.C. (1988) On the Nonlinearity of the Tropospheric Ozone Production, *J.Geophys. Res.*, **93**, No. D12, pp 15879-15888.
- Lindskog, A. (1996) *Nonmethane hydrocarbons and nitrogen oxides in background air. Long range transport of precursors in relation to oxidant formation*. Doctoral thesis. Department of analytical chemistry, Stockholm University, Sweden.
- Lindskog, A. (1997) Swedish Environmental Institute (IVL), Göteborg, Sweden, Personal communication.
- Mylona S. (1996) Emissions, The collation and nature of emission data, in EMEP/MSC-W Report 1/96, Barrett, K. and Berge. E. (Eds), The Norwegian Meteorological Institute, Oslo, Norway.
- Pleijel, K. and Andersson-Sköld, Y. (1992) Jämförelse mellan olika kemiska modeller för tillämpning vid regional simulering av luftföroreningar, Swedish Environmental Research Institute (IVL) Report B-1048 (in Swedish), Göteborg, Sweden.
- Pleijel, K., Andersson-Sköld, Y. and Ohmstedt, G. (1992) Atmosfärkemiska och meteorologiska processers betydelse för mesoskalig ozonbildning, Swedish Environmental Research Institute (IVL) Report B-1056 (in Swedish), Göteborg, Sweden.
- Poppe, D., Andersson-Sköld, Y., Baart, A., Builtjes, P., Das, M., Hov, Ø., Kirchner, F., Kuhn, M., Makar, P.A., Milford, J.B., Roemer, M., Ruhnke, R., Simpson, D., Stockwell, W.R., Strand, A., Vogel, B. and Vogel H. (1996) Gas-phase reactions in atmospheric chemistry and transport models: a model intercomparison, the

- Chemical Mechanism Working Group (CMWG) within EUROTRAC,  
EUROTRAC International Scientific Secretariat, Garmisch-Partenkirchen.
- Sillman S. (1995) The use of  $\text{NO}_y$ ,  $\text{H}_2\text{O}_2$  and  $\text{HNO}_3$  as indicators for ozone- $\text{NO}_x$ -hydrocarbon sensitivity in urban locations, *J. Geophys. Res.*, **100**, No. D7, pp 14175-14188.
- Sillman S. (1997) Department of Atmospheric, Oceanic, and Space Sciences, University of Michigan, Ann Arbor, USA, personal communication.
- Sillman S. and Samson P. J. (1993) Nitrogen oxides, regional transport, and ozone air quality: results of a regional-scale model for the midwestern United States, *Wat. Air Soil Pollut.* **67**, 117-132.
- Sillman S., Logan J.A. and Wofsy S.C. (1990) The Sensitivity of Ozone to Nitrogen Oxides and Hydrocarbons in Regional Ozone Episodes, *J. Geophys. Res.*, **95**, No. D2, pp 1837-1851.
- Simpson, D. and Hov, Ø. (1990) Long period modelling of photochemical oxidants in Europe. Calculations for July 1985. EMEP MSC-W, The Norwegian Meteorological Institute, P.O. Box 43 - Blindern, N-0313 Oslo 3, Norway.
- Simpson, D., Andersson-Sköld, Y. and Jenkin, M.E. (1993) Updating the chemical scheme for the EMEP MSC-W oxidant model: current status, EMEP MSC-W Note 2/93.
- Staffelbach T., and Neftel A.(1996) On the VOC or  $\text{NO}_x$  limitation of ozone formation over Southern Switzerland: Experimental and model results, *EUROTRAC newsletter*, No. 17, pp 18-21.
- Stockwell, W.R., Middleton, P. and Chang, J.S. (1990) The second generation regional acid deposition model chemical mechanism for regional air quality modelling, *J. Geophys. Res.*, **95**, No. D10, pp 16343-16367.
- Taesler (1972). Climatic data for Sweden ( in Swedish). ISBN 91-540-2012-3. SMHI, Norrköping, Sweden.



---

**IVL Svenska Miljöinstitutet AB**

Box 210 60, SE-100 31 Stockholm  
Hälsingegatan 43, Stockholm  
Tel: +46 8 598 563 00  
Fax: +46 8 598 563 90

[www.ivl.se](http://www.ivl.se)

**IVL Swedish Environmental Research Institute Ltd**

Box 470 86, SE-402 58 Göteborg  
Dagjänningsgatan 1, Göteborg  
Tel: +46 31 725 62 00  
Fax: +46 31 725 62 90

Aneboda, SE-360 30 Lammhult  
Aneboda, Lammhult  
Tel: +46 472 26 20 75  
Fax: +46 472 26 20 04